

AL04 - Cathode Cooling Damages Due to Potline Power Interruptions

Alton Tabereaux¹ and Marc Dupuis²

1. Consultant, Muscle Shoals, AL, USA 35661

2. Genisim Inc., 3111 Alger St., Jonquiere, Québec, Canada G&S 2M9

Corresponding author: marc.dupuis@genisim.com

Abstract

Prolonged electrical power interruptions often result in the shutdown of aluminum cells in potlines. Cooling cells to ambient temperature causes irreversible and non-repairable damage to the carbon cathode lining due to the formation of numerous, and often deep, cooling cracks on the top surface of cathode blocks and in rammed seams between blocks that ultimately shorten potlife. In this work, ANSYS® 12.0 based 3-dimensional full cell quarter and 3D slice thermal cooling models results provide verification that large tensile stresses are generated in the cathode panel due to the bottom face of the cathode being anchored by steel collector bars while the top of the cathode panel is shrinking during cooling. It was found that after 24 hours of cooling the thermo-mechanical stress generated at the top surface of the cathode panel was greater than 11 MPa which is enough to cause cracks in the cathode panel occurring at around 8 MPa.

Keywords: Modeling, cooling, thermomechanical, cathode cracks.

1. Introduction

Carbon cathode and anodes used in industrial aluminum cells are submitted to thermomechanical stresses at different times in their life, for example while pouring molten cast iron into the cathode block slots to hold steel collector bars in place, heating cells for startup, at immersion of new anodes into molten bath and when cooling pots to ambient once the electrical current is interrupted.

The duration of power outages during a power interruption determines the extent of cooling of the bath, which in turn determines how many pots will be shut down due to frozen cryolytic bath, and therefore the number of pots that will have damaged cathodes. Cooling occurs in all cells in a potline when the electrical power is interrupted. The internal pot Joule (I^2R) heating stops in all pots; however, pots initially continue to dissipate heat at the same rate as during normal operations. Pots cool at different rates due to differences in their size, lining design and operating parameters. Modern cells lose heat at a faster rate compared with older cell technologies due to their use of more thermal conductive cathode construction materials and, therefore, are at a higher risk of shutting down due to power interruptions.

Cooling cells to ambient temperature can cause irreversible and non-repairable damage to the carbon cathode lining. For example, the formation of numerous, often deep, cooling cracks on the surface of cathode blocks and in the rammed seams between blocks has been consistently observed, with a resulting shortened potlife when the cell is restarted.

1.1. Thermal Arrest

A thermal arrest is a significant phenomenon in aluminum cells during long power interruptions because it decelerates the cooling process which slows the increase in electrical resistance of the bath and maintains liquid some cryolytic electrolyte which helps when reenergizing power in the potline once power is restored. In some instances, the thermal arrest delay in cooling has assisted

some potlines to continue operating after 6 to 8 hours of power interruption by keeping the cryolitic bath molten longer.

Aluminum electrolysis cells typically operate in the range 955 to 965 °C depending on chemistry and superheat. Solidification of cryolitic bath in cells begins when the bath temperature in cells cools to its freezing point, 940 to 950 °C depending on chemistry. Cryolitic bath typically cools at a rate of 15–20 °C per hour, depending on cell heat losses, until further cooling is temporarily halted due to a phase change from liquid to solid with evolution of the latent heat of fusion. This is the energy required for a phase change which keeps the remaining liquid at the freezing temperature until nearly all the liquid has solidified. Cooling the electrolyte in cells below ~850 °C results in the solidification of the totality of the bath.

The length of time for the thermal arrest depends largely on the volume of liquid bath in the cell, heat losses, and chemistry. It is expected that molten cryolite freezes at the outset near the sides and ends of cells which are also the locations of highest heat loss, and finally freezes in the center of the cell.

1.2. Thermal Arrest During a 5-Hour Power Interruption in a 300 kA Potline

A 5-hour power interruption occurred due to a power failure in 2008 in a 300 kA pot line with 160 cells at the Keao Aluminum Company in Zoucheng, China [1]. Bath temperatures were measured hourly; they decreased rapidly from 967 °C to around 920 °C where the cooling halted for about 1 hour at a thermal arrest due to the freezing of molten cryolite as shown in Figure 1.

The average temperature of the molten bath in four cells after 4 hours of cooling was 897 °C. The 1-hour thermal arrest slowed the cooling process which halted the decrease in temperature for 1 hour, thus reducing the electrical resistance of the bath and retaining liquid cryolite which greatly aided restoring operations when reenergizing the potline once power was restored.

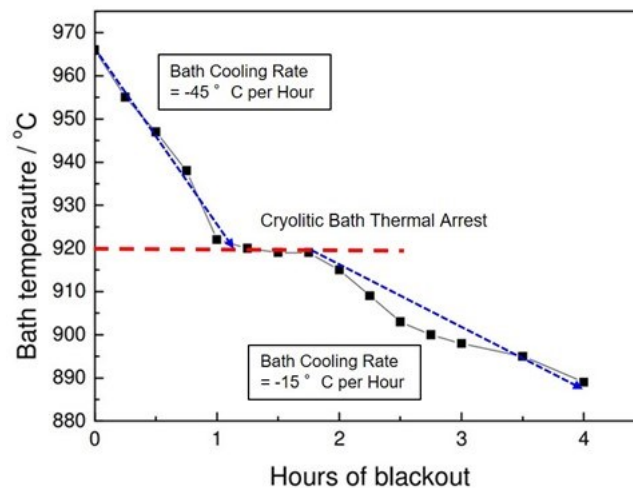


Figure 1. Bath cooling temperatures with a 1-hour thermal arrest at 920 °C during a 5-hour power interruption.

Most of the cells in the potline continued to operate after the potline was reenergized. At that time, cells operated at low amperage, 120 kA. Bath was generated in some cells by operating at 10 V which increased the thermal input and thereby increased the melting of cryolite and solid bath in a few cells. After 2 weeks, the metal purity was greater than 99.7 %, indicating that the

cathodes in cells did not fracture and form cracks because the cell temperature was greater than 880 °C during the 5 hours of cooling.

1.3. Thermal Arrest During an 8.5-Hour Power Interruption in a 200 kA Potline

An 8.5-hour power interruption occurred due to a transformer failure in 1985 at the Reynolds aluminum smelter in Baie Comeau, Canada; 229 out of a total of 240 cells in the 200 kA potline continued to operate after the potline was reenergized. Bath temperatures were measured in two pots during the 8.5-hour power outage as shown in Figure 2. After 6 hours of power outage, the cryolitic bath temperature decreased to 870 °C and remained nearly constant at a thermal arrest for about 3 hours due to the phase change from liquid to solid with evolution of the latent heat of fusion [2].

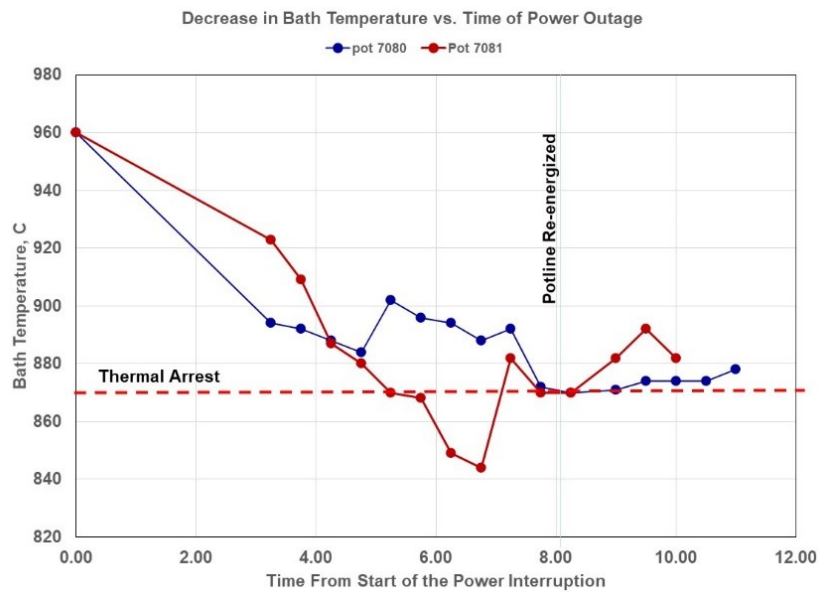


Figure 2. Bath cooling temperatures with a 3-hour thermal arrest at 870 °C during an 8.5-hour power interruption.

At that point, an inversion with mixing of molten bath and liquid aluminum occurred. Anodes were lowered manually with a wrench in 1 cm in 85 pots during the power outage, and then in all pots, to contact liquid aluminium to provide *hibernation* heating of approximately 2.0 V per pot once power was restored to the potline. Nine pots were stopped after reenergizing the potline due to operational problems associated with anode transition joint failures [5].

1.4. Solidification of Aluminum During Cooling

After molten cryolite freezes, cooling continues in industrial cells until the liquid aluminum solidifies at its melting point of 660 °C. Measurements of the cooling temperature of liquid aluminum in a 100 kA prebake cell at the Alcoa Rockdale aluminum smelter after power is stopped indicates that a thermal arrest in cooling occurs when the decreasing temperature of liquid aluminum halts at its solidification temperature 660 °C for 4 hours as shown in Figure 3 due to the phase change of 5 tonnes of liquid to solid aluminum [3]. The latent heat of solidification required for the phase change heat keeps the remaining liquid aluminum at its freezing temperature until nearly all the liquid aluminum has solidified. Measurements of aluminum at six different locations in the cell confirmed that the metal solidified first at the sides and ends of the cells and last in the center of the cell. It was estimated that with removing the anodes after 24

hours, the aluminum at the center of the cell will freeze completely in 31 hours after the cell is removed from line current.

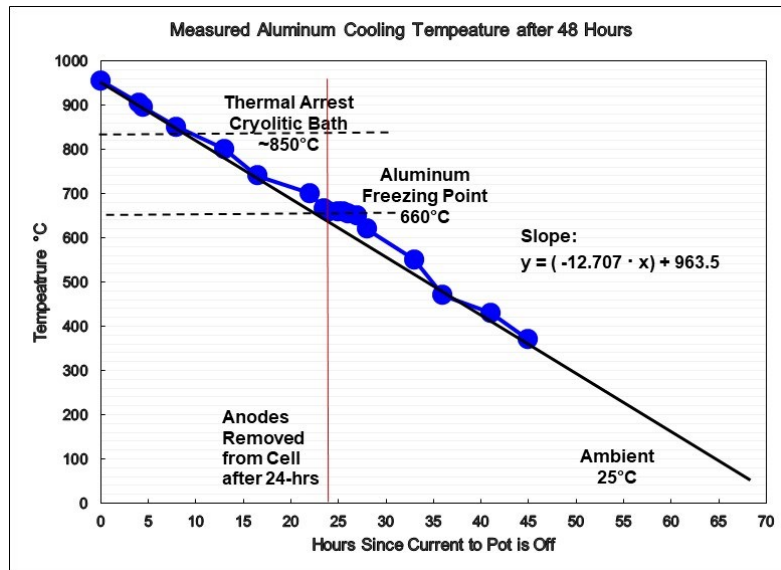


Figure 3. Liquid aluminum cooling temperatures with 4-hour liquid aluminum solidification thermal arrest at 660 °C.

After the aluminum is solidified, the cathode continued cooling at rate of 8 °C per hour to ambient in about 3 days. High amperage cells have larger cathodes that contain 15 to 40 tonnes of molten aluminum depending on the size of the cathode required for its operating amperage. Large prebake cells may take from 5 to 7 days to cool to ambient [4]. In the early 2000's, it was common for smelters to put water on cathodes to increase the cooling rate. Watering substantially reduced the turnaround time for relining cathodes, made it easier to dig the cathode materials from the steel potshell and, in some instances, made it easier to process the cathode materials at the SPL processing plant.

2. Cathode Damages as a Result of Cooling

The thermomechanical behavior of cathode carbon materials has been described as elasto-plastic [5]. Initially, cathode carbon blocks behave elastically, with reversible deformation as stress is applied. When the stress continues to increase, cathode materials starts to behave in a more plastic manner and undergoes irreversible deformation until fracture occurs. Cathode blocks are significantly weakened by micro-cracking produced by the diffusion of sodium into the carbon lattice during electrolysis. Stresses in cooling cathodes are generated by thermal gradients and by restraining their free thermal contraction.

2.1. Cathode Cracks Due to Cooling

It has been demonstrated that cooling aluminum cells from 960 °C to ambient 25 °C results in the initiation of cracks on the top cathode panel surface of nearly all cells. The cracks can be observed when the metal pad is removed, and the surface cleaned for inspection. The cracks are formed on the top surface of the cathode panel during cooling; they are not present during cell operation as indicated by the clean black surfaces inside new cracks as shown in Figure 4. A yellow film of aluminum carbide was generated during past cell outages of cells cooled to ambient. The width of observed cooling cracks observed is from 1.6 to 3 mm; they often extend the length of the cathode blocks, ~300 cm and can be deep as shown in Figure 4. The distances between cooling cracks vary widely in the cathode panel but are typically found to occur about two cathode blocks

apart [6]. Cracks are a major cause for the decrease in potlife when pots are stopped and cooled to ambient. Once a cathode has developed cracks, gaps, etc. there is no known method to repair the damage.

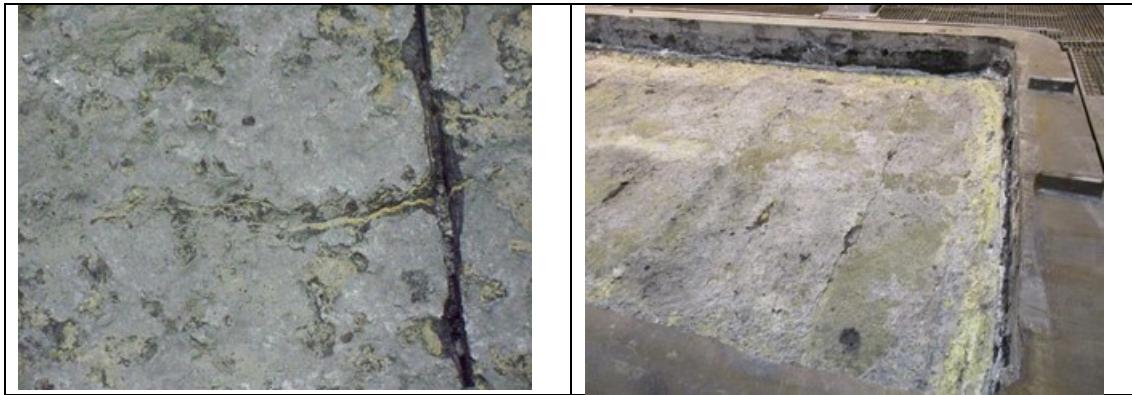


Figure 4. Cooling cracks on the top surface of the cathode panel.

2.2. Cathode Shrinkage as a Result of Cooling

During 4 to 8-hour power interruptions, the temperature of industrial aluminum cells cools down around 110 degrees to the thermal arrest, (850 °C); when the potline is reenergized, cells heat up to 960 °C without cathode damage as confirmed by the metal purity, cathode voltage drop, cell stability, and normal potlife. However, cells that are cooled 935 degrees to ambient, (25 °C) result in damages and loss in potlife that are associated with cathode cooling cracks.

The 9 m long cathode panel of a 200 kA prebake cell, with 12 cathode blocks, expands 3.0 cm in length when heated from ambient to the operating temperature, 960 °C. During extended cooling, the cathode panel shrinks 0.3 cm in length after cooled 110 degrees to the thermal arrest temperature of cryolite, (850 °C); shrinks 0.9 cm after cooled 300 degrees to the solidification temperature of liquid aluminum, (660 °C); and shrinks 3.0 cm after cooled 935 degrees to ambient temperature, 25 °C as shown in Figure 5.

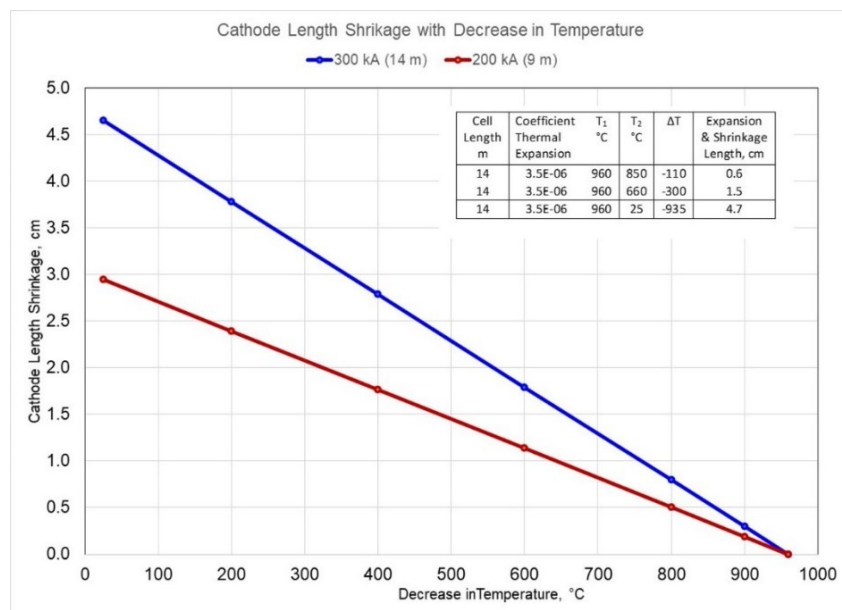


Figure 5. Cathode length shrinkage with decrease in temperature for 200 and 300 kA cells.

By comparison, the 14 m long cathode panel of 300 kA prebake cells, with 20 cathode blocks, expand 4.7 cm in length after heated from ambient to operating temperature, 960 °C, and shrinks the same distance after cooled to ambient. Shrinkage occurs first on the top section of the cathode blocks, as this section cools down faster through the metal pad. Furthermore, the bottom section is anchored by 80 steel collector bars in the 20 cathode blocks, 4 bars per cathode block preventing it to freely shrink.

2.3. Fracture Behavior of Cathode Materials

Carbon cathode and anodes used in industrial aluminum cells are submitted to thermomechanical stresses at different times in their life, for example during pouring molten cast iron into the cathode block slots to hold steel collector bars in place, heating cells for startup, immersion of new anodes into molten bath and cooling pots to ambient when the electrical current is interrupted.

In 1991 Allard et.al and other researchers stated that the mechanical fracture behavior of different kinds of cathode carbon materials ranging from anthracitic to fully graphitized have been identified in three-point bending tests as elasto-plastic [7, 8]. Cathode materials are often described as brittle, but they have been found to be heterogeneous and their fracture behavior is not (quite) brittle, but rather quasi-brittle. This means they can withstand a certain damage, like a crack, without breaking at once. Cathode blocks initially behave elastically with reversible deformation as stress is applied, but when stress increases, the carbon material starts to behave in a plastic manner with irreversible deformation until fracture occurs, for example in cathode block heaving, or arching, in cells.

In 2000, Allard et.al found, when measuring flexural strength of cathode materials, that the load displacement curves indicates that cathode materials can exhibit brittle or non-brittle behaviors, depending on graphite grades [9]. Brittle cathode materials exhibit a linear load-displacement curve up to 400 μm and the fracture is catastrophic and non-brittle materials exhibit a slight non-linear load displacement curve up to 400 μm and the failure is less abrupt.

Cathode heaving is an example of cathode blocks arching that occurs due to the cathode material slowly deforming permanently under the influence of persistent mechanical stresses due sodium concentration gradients or push-up due to formation of voluminous reactions products under blocks. Cathode heaving can result in 6 to 10 cm arching in the center of blocks with eventual cracking and failure of the cathode lining in the cell.

Flexural strength, also known as modulus of rupture or bending strength is a material property that represents the highest stress experienced within the material at its moment of a brittle fracture, or at the moment of the highest sustained load for a quasi-brittle fracture. The transverse bending test is most frequently employed, in which a specimen having either a circular or a rectangular cross-section is bent until fracture, using a three or a four points flexural test technique.

Composition of Cathode Blocks

The difference in composition and manufacturing temperatures of cathode blocks used in industrial aluminum cells are shown in Table 1. Graphitized blocks are the most expensive due to their processing costs, but they have the lowest electrical resistance which significantly reduces the cell operational energy consumption. They have the highest tensile strength at 980 °C, as well as the greatest resistance to sodium expansion during electrolysis. Graphitized blocks have the highest thermal conductivity which reduces the temperature gradients during cooling and reduce brittle transformation and permanent plastic deformation. However, graphitized blocks have the highest rate of cathode surface erosion wear, especially at locations near the end of each block due to higher current density at that location. Semi-graphitized blocks provide most of the same

advantages as graphitized cathode blocks but are less expensive. Graphitic blocks are intermediate in all cathode properties. Anthracite blocks are the least expensive, they have high crushing strength and low erosion wear rates but they have the least resistance to sodium adsorption, migration, and intercalation in blocks during electrolysis. They also have the highest electrical resistance.

Table 1. Composition of Cathode Blocks.

Cathode Block	Composition and Manufacturing Temperature
Anthracite or Amorphous	100 % Anthracite coal plus pitch binder; blocks are baked to 1 200 °C.
Graphitic	Aggregate consisting of both anthracite and 30–50 % graphite plus pitch; blocks are baked to 1 200 °C.
Semi-graphitized	Petroleum coke plus pitch; blocks are baked to an intermediate level temperature from 2 100 to 2 400 °C.
Graphitized	Petroleum coke plus pitch; blocks are graphitized in an electric furnace from 2 900 to 3 000 °C.

Thermomechanical Properties of Cathode Materials at 25 °C

The mechanical properties of the cathode blocks are dependent upon macro-anisotropy of the blocks as the effect of grain orientation on flexural strength is significant in extruded cathode blocks. Cracks parallel to the direction of extrusion of anthracitic cathode blocks require less fracture energy, 103 J/m², than cracks perpendicular to extrusion, 126 J/m² [7]. When the grains are perpendicular to crack formation, it requires higher energy either to pass around the grain or break it if it is too long.

The thermomechanical properties of various types of cathode block materials measured at 25 °C by Allard et.al are shown in Table 2 [7, 9, 10]. The flexural strength, the maximum bending stress required to fracture semi-graphitic, graphitic and graphitized materials was from 8 to 9 MPa compared with 7 MPa for anthracitic materials measured in the parallel direction. The compressive strength, the capacity of a material or structure to withstand compressive loads tending to reduce size, was significantly higher for anthracite materials, 34 MPa, compared with only 24 MPa for graphitized materials.

Table 2. Thermomechanical Properties of Cathode Block Materials at 25 °C.

Cathode Material	Graphite %	Flexural Strength ¹ (MPa)	Flexural Strength ² (MPa)	Fracture Energy (J/m ²)	Young Modulus (GPa)	Compressive Strength (MPa)
Anthracite	0	7 [7, 9]	n/a	126 [7] 166 [9]	11 [7, 9]	34 [7]
Semi-graphitic	30	9 [7, 9] 8 [10]	8 [10]	123 [7] 166 [9, 10]	10 [7, 9]	29 [7]
Semi-graphitic	50	9 [7, 9]	n/a	131 [7] 191 [9]	10 [7]	27 [7]
Graphitic	100	9 [7, 9] 8 [10]	8 [10]	137[7] 177 [9, 10]	8 [7]	26 [7]
Graphitized	100	10 [10]	9 [10]	255 [10]	7 [7]	24 [7]

¹Parallel, ²Perpendicular; [7] Allard 1991, [9] Allard 1995, [10] Allard 2000.

The Young's modulus, the stiffness of a solid material, was higher for anthracite materials, 11 GPa, compared with only 7 GPa for graphitized materials. The fracture energy, the amount of energy required by a crack to propagate in the material, was significantly higher for graphitic materials, 255 J/m², compared with 126–166 J/m² for anthracite materials.

The thermomechanical properties of various types of cathode block materials measured at 1 000 °C are shown in Table 3 [9–11].

Allard et.al determined that a flexural stress higher than 10 to 11 MPa is needed to fracture anthracitic, semi-graphitic and graphitic cathode block materials at 1 000 °C. A higher stress, 13 MPa, is required to fracture graphitized cathode materials. The flexural strength was consistently 3 MPa higher in the parallel direction compared with the perpendicular direction for the anthracitic and semi-graphitic cathode materials but almost the same for graphitic and graphitized cathode materials.

The Young’s modulus was 10–12 GPa at 1 000 °C for anthracitic and semi-graphitic materials which is about the same as measured at 25 °C. The fracture energy measured at 1 000 °C was higher for graphitic materials, 269–299 J/m² compared with 212–234 J/m² for anthracite and semi-graphite materials.

Picard et.al measured the Young’s modulus and compressive strength at 1 000 °C for graphitic and graphitized materials [11]. The compression strength for graphitic cathode material increased around 28 % from 25 MPa to 32 MPa over the range of 25 °C to 1 000 °C and the corrected value for the Young’s modulus of graphitic material decreased from 8 to 6 MPa at 800 °C. The uniaxial compressive strength for graphitized cathode material increased from 24 GPa to 32 GPa over the range of 25 °C to 1 000 °C, and the corrected value for the Young’s modulus of graphitized material decreased from 7 to 6 GPa at 800 °C.

Table 3. Thermomechanical Properties of Cathode Blocks at 1 000 °C.

Cathode Material	Graphite %	Flexural Strength ¹ (MPa)	Flexural Strength ² (MPa)	Fracture Energy ¹ (J/m ²)	Fracture Energy ² (J/m ²)	Young’s Modulus (GPa)	Compressive Strength (MPa)
Anthracite	0	10 [9]	7.0 [9]	234 [9]	241 [9]	12 [9]	n/a
Semi-graphitic	30	11 [9]	8.0 [9]	212 [9] 212 [10]	153 [9] 153 [10]	10 [9]	n/a
Graphitic	100	10 [9]	7 [9]	314 [9] 306 [10]	179 [9] 178 [10]	6 [11]	32 [11]
Graphitized	100	13 [10]	11 [10]	299 [10]	269 [10]	6 [11]	32 [11]

¹Parallel, ²Perpendicular; [9] Allard LM 1995, [10] Allard LM 2000, [11] Picard 2010.

The flexural strength of various types of cathode materials measured after 6 to 13 hours of electrolysis at 980–1 000 °C is shown in Table 4 [11, 12].

Welch et.al measured the flexural strength of anthracitic, semi-graphitized and graphitic cathode materials after 7 to 13 hours of electrolysis [12]. The sodium absorption by anthracitic materials during electrolysis led to a 50 % loss of flexural strength as the flexural stress necessary to fracture anthracitic cathode materials was reduced by 50 % from around 8 MPa to about 4 MPa after the first hour of electrolysis. By comparison, the strength of graphitic material decreases by 17 % from 12 MPa to 10 MPa and the strength of the graphitized material is unaffected after electrolysis.

Hop et.al measured the flexural strength of semi-graphitic, graphitic and graphitized cathode materials after 6 hours of electrolysis at 980 °C [13]. The strength of the semi-graphitic block material (anthracite plus 30% graphite) lost > 50% of its flexural strength in the first hour of electrolysis but recovered to around 12 MPa after three hours of electrolysis. Two graphitic cathode materials lost strength after the first hour of electrolysis, from 12–13 MPa to 6–9 MPa

but recovered to 12–15 MPa. The strength of the graphitized cathode material was unaffected after 6 hours of electrolysis as it retained its high strength of 20 MPa at 980 °C.

Table 4. Flexural Strength of Cathode Blocks After Electrolysis at 980–1 000 °C.

Cathode Material	Graphite %	Test Hours	Flexural Strength MPa
Anthracite	0	7, [13]	4 [11]
Semi-graphitic	30	7, [13]	6 [11] 10 [12]
Graphitic	100	6, [13]	8 [11] 10 [12]
Graphitized	100	6	20 [12]

[12] Welch 1991, [13] Hop 2004.

In summary, the flexural strength tests by several investigators to date indicate that:

- A tensile stress greater than 8 MPa is required to cause fracture of semi-graphitic and 100 % graphitic cathode blocks at 25 °C and 1 000 °C in the parallel direction.
- A tensile stress greater than 10 MPa is required to cause fracture of graphitized cathode blocks at 25 °C and 1 000 °C in the parallel direction.
- The flexural strength was lower for all types of blocks in the perpendicular direction at 25 °C and 1 000 °C.
- The flexural strength was significantly reduced > 50 %, in anthracite cathode blocks after one hour of electrolysis at 980 °C and to a lesser extent in the semi-graphitic cathode blocks.
- The flexural strength of the graphitized cathode blocks was unaffected by electrolysis.

3. Modeling Thermo-mechanical Stresses in Aluminum Cell Cathodes During Cooling

In the present work, coupled thermo-mechanical ANSYS® 3-dimensional FEM models were developed to analyze both the cooling rates, the difference in temperature gradients and the resultant stresses in 360 kA aluminum cell cathodes during cooling. These stresses can lead to fracture and propagation of cracks in cathode blocks that result in irreversible and irreparable damage of the cathode.

As reported by Dupuis and Tabereaux, the ANSYS® based full cell quarter thermal model provides more accurate results than slice cell models as it includes the effect of all of the external cell heat loss surfaces, including the pot shell end wall, cradles, alumina-bath cover on anodes, and the anode assembly including individual anode stubs, yoke and rods [14].

The thermal solution determined for a 3D full quarter thermal model of a 360 kA cell with graphitized cathode blocks is shown in Figure 6 after 48 hours of cooling of the cathode lining. The maximum temperature of 673 °C indicates that the molten cryolitic bath is frozen, and the aluminum metal started to solidify at 660 °C.

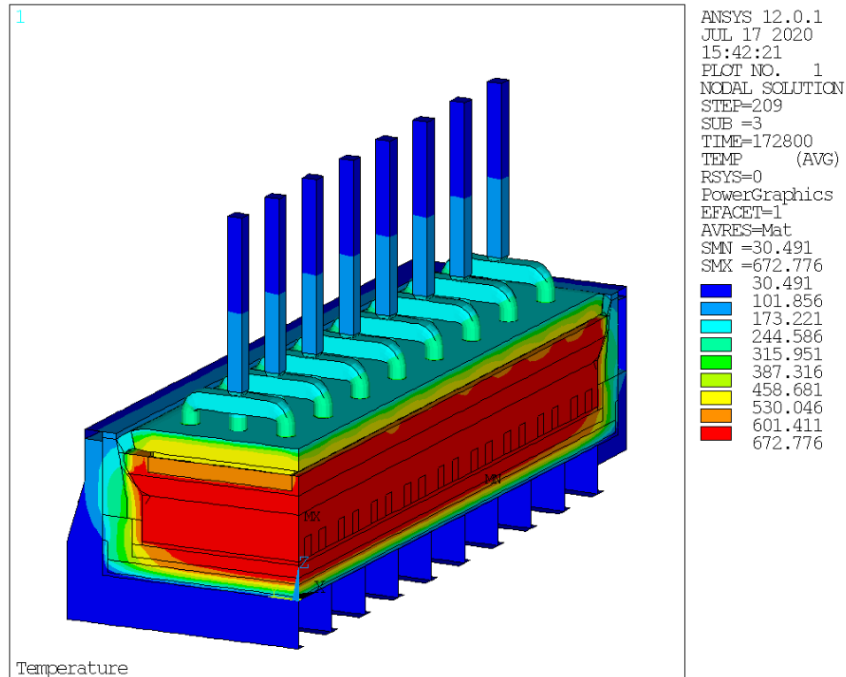


Figure 6. 3-Dimensional full cell quarter thermal cooling model of a 360 kA cell (temperature solution after 48 hours of cooling).

Temperature Distribution in the Cathode Panel after 24 hours of Cooling

To obtain faster results, a mix of individual cathode slice models and quarter cathode panel models were utilized to obtain results of cathode cooling rates, temperature distribution and stresses during 24-hour and 48-hour cooling for 30 % graphite (graphitic) and 100 % graphite (graphitized) cathode blocks. Thermal mechanical solutions were obtained nearly continuous cathode cooling temperatures and stresses for 24 and 48 hours of cooling.

The scale of the distribution of temperatures of only the cathode *panel* with 30 % graphite cathode blocks after 24 hours of cooling is shown in Figure 7 left. Temperatures vary from the minimum value of 541 °C at the anchored bottom section of the panel to a maximum value of 852 °C at the top surface of the panel, a thermal gradient difference of 311 °C.

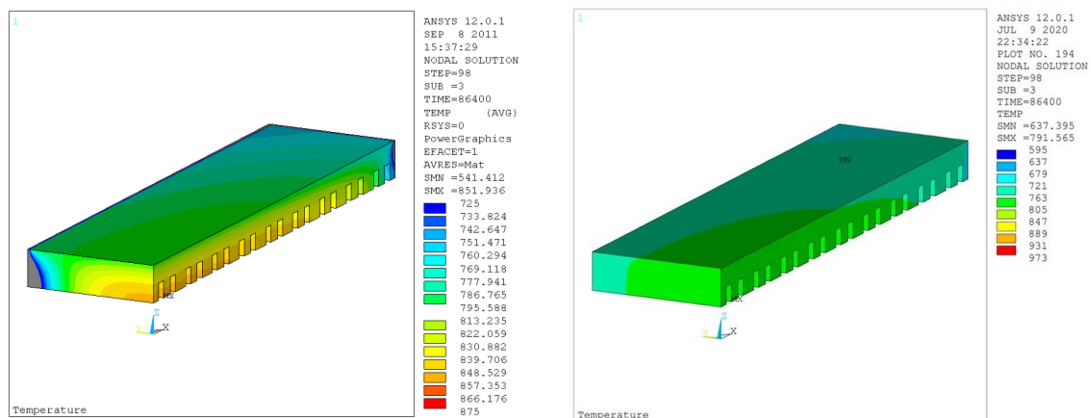


Figure 7. Temperature Distribution of 3D Cathode Panels after 24 hours cooling. Left: 30 % graphite cathodes, Right: 100 % graphite cathodes.

By comparison, the temperatures in the graphitized (100 % graphite) cathode panel after 24 hours of cooling, shown in Figure 7 right, vary from the minimum value of 637 °C at the anchored bottom section of the panel to a maximum value of 791 °C at the top surface of the panel, a thermal difference of 154 °C.

The difference between the temperatures at the top and bottoms sections of the cathode panel after 24 hours cooling is shown in Figure 8. The difference in temperatures for 30 % graphite cathodes varies from the minimum value of -112 °C at the anchored bottom section of the panel to a maximum value of -248 °C at the top surface of the panel, a thermal difference of 136 degrees.

The difference in temperatures for 100 % graphite cathodes varies from the minimum value of -160 °C at the anchored bottom section of the panel to a maximum value of -239 °C at the top surface of the panel, a difference of only 79 degrees. The lower difference in top-bottom temperatures in graphitized cathode blocks is significant as the lower thermal gradient reduces the thermal-mechanical stress in the cathode blocks. The difference between min and max temperature is different between Figures 7 and 8 because there is also a thermal gradient in the cathode block operating temperature.

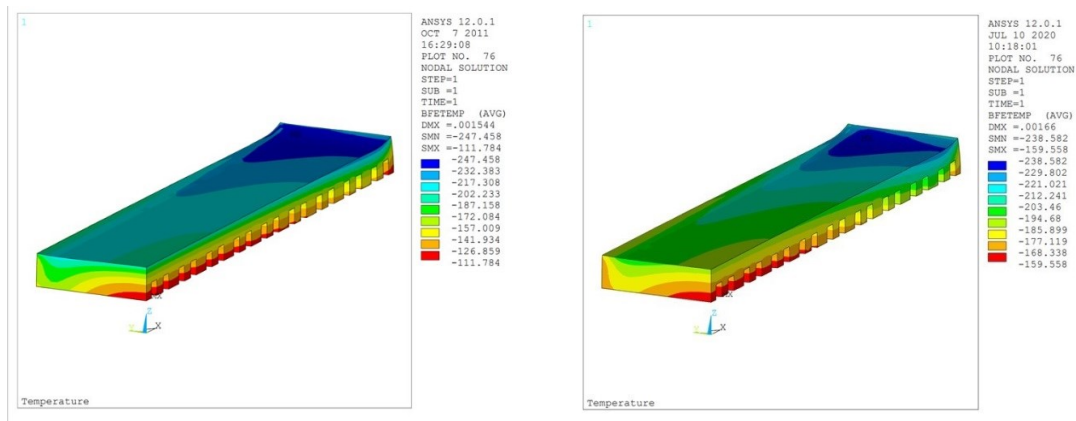


Figure 8. The average difference in temperatures at the top and bottoms sections of the cathode panel after 24 hours cooling: Right: 30 % graphite cathodes, Left: 100 % graphite cathodes.

It is readily apparent that the lower cathode panel temperatures in the graphitized cathode panel is due to higher heat losses because of the higher thermal conductivity of the graphitized material, 100 W/m K at 1 000 °C. However, it has established that 30 % graphite block material becomes more graphitized during electrolysis.

3.1. Thermal Gradients in the Cathode Panel

It is assumed that at time zero in steady state operating condition, the cathode block is stress free under no mechanical constrains. As cooling proceed, the thermal load that will be used to carry the thermo-mechanical study is the differential temperature between the current thermal condition and the initial steady-state thermal conditions as presented in Figure 9.

The top of the cathode blocks cools faster than the bottom section of the cathode panel, as shown in Figure 9. A large stress is generated in the cathode panel, that is produced by the non-uniform shrinkage of the cathode blocks caused by the thermal gradient of the differential temperature in blocks.

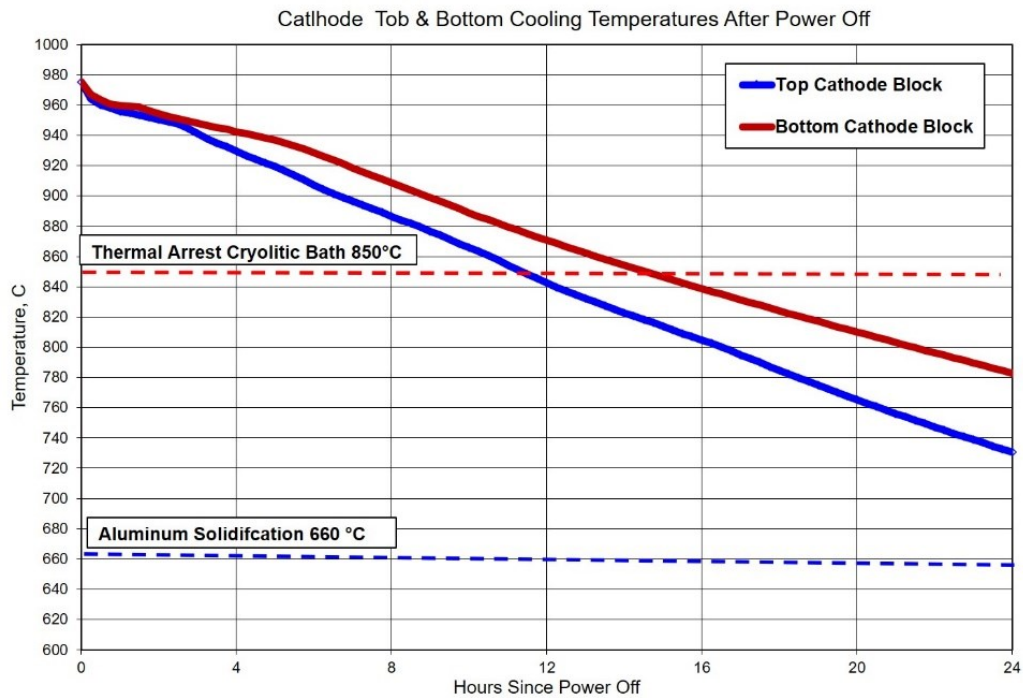


Figure 9. Cathode cooling curves for top and bottom of cathode panel.

When an object formed of a single material like a beam is bent, it experiences a range of stresses across its depth. At the edge of the object on the inside of the bend (concave face) the stress will be at its maximum compressive stress value. At the outside of the bend (convex face) the stress will be at its maximum tensile value. Most materials fail under tensile stress before they fail under compressive stress, so the maximum tensile stress value that can be sustained before the beam fails is its flexural strength. The flexural strength would be the same as the tensile strength if the material were homogeneous. Dupuis and Tabereaux demonstrated that this mechanism alone is not enough to produce enough tension stress to induce fractures on the top surface of the cathode [14].

3.2. Thermal Stress at the Top Surface of the Cathode Panel with the Bottom of the Cathode Panel Anchored

According to Dupuis and Tabereaux, the bottom of the cathode panel in aluminum cells is anchored by steel cathode bars at the windows through the potshell; the top surface of the cathode panel cools faster than the bottom section of the cathode panel, and is free to shrink as the temperature of the aluminum cools during extended power interruptions causing tension stress in the top surface of the cathode [15]. The addition of the bottom anchoring to the thermal gradient produces additional tensile stresses on the top surface of the cathode.

The distribution of stresses in the long direction on the cathode panel after 24 hours of cooling, which is the X direction for the 3D model, are presented in Figure 10. Positive numbers indicate tension while negative values indicate compression. Cathode blocks will crack under tension. Tension stress varies from 0 MPa at the bottom surface of the panel to the maximum 11 MPa at the top surface of the panel. The high maximum value exceeds the 8 MPa stress determined for fracture and crack propagation of cathode block materials.

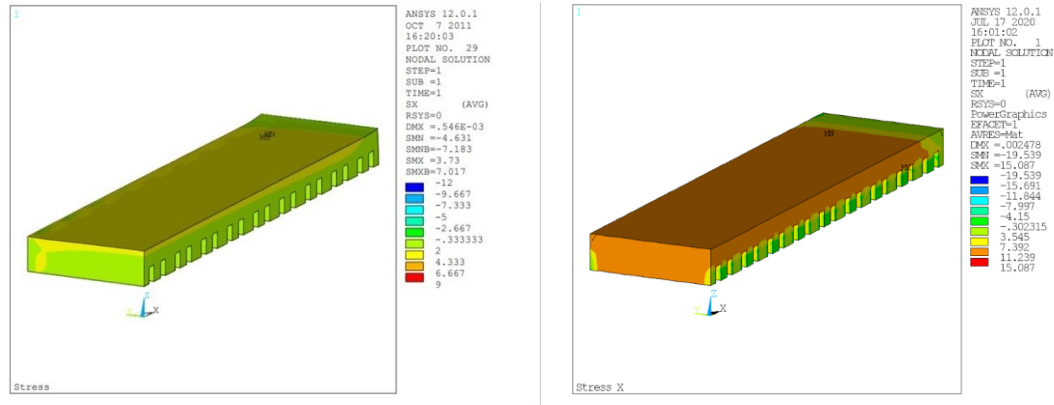


Figure 10. Cathode panels after 24 hours cooling. Left: Stress due to thermal gradient only [14]. Right: Thermo-mechanical stress, due to thermal gradient and collector bars anchoring.

3.3. Tensile Stress Evolution during Cooling

ANSYS modeling results indicate that the thermo-mechanical stress increases linearly up to 20 hours after power is off in aluminum cells due to the cooling of the cathode panel which is in contact with the aluminum metal pad as shown in Figure 11.

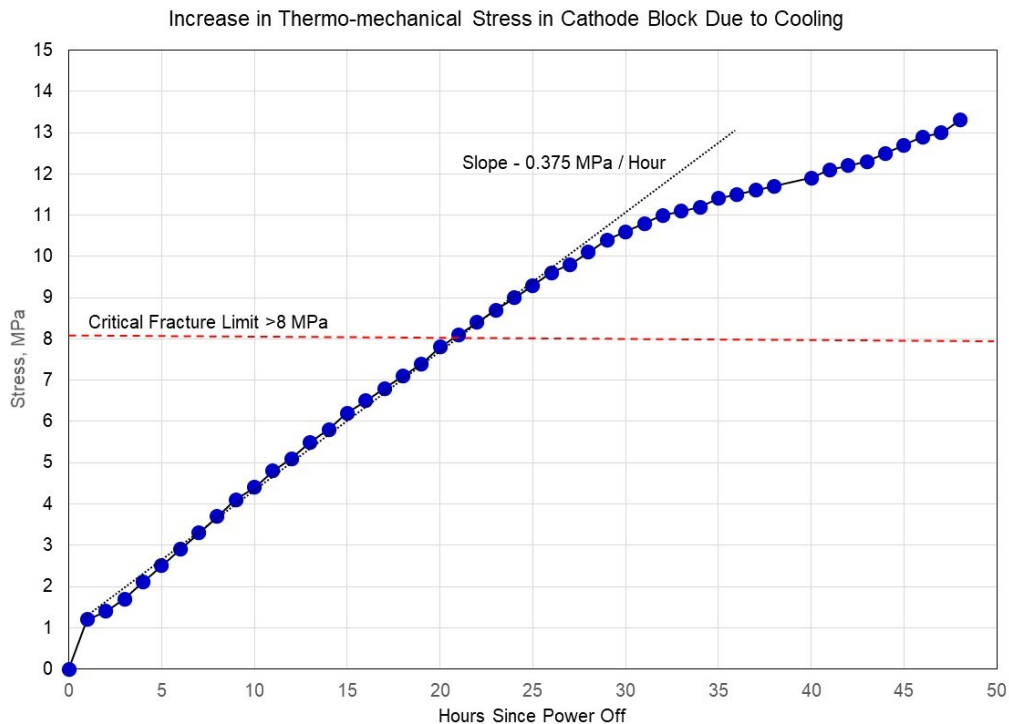


Figure 11. Thermo-mechanical stress in cathode blocks due to cooling.

The tensile stresses in the carbon cathode panel increases at a linear rate of 0.375 MPa per hour until 25 hours of cooling when the temperature of the cathode block is impacted by the thermal arrest due to solidification of aluminum at 660 °C and increase in the heat of fusion of the aluminum metal in contact with the top surface of the cathode panel.

After 20 hours of cooling, the stress exceeds the critical limit of 8 MPa to cause cathode cracks. Hence, the thermo-mechanical stress in aluminum cells with power interruptions less than 10 hours would be insufficient to cause cooling cracks in the cathode panel.

3.4. Cathode Damages

Aluminum cells are damaged due to fracture of cathode blocks when cooled from 960 to 25 °C. Numerous measurements shown in Tables 2 and 3 have verified that the thermo-mechanical flexural stress must be > 8 MPa to cause fracture in all types of cathode blocks except anthracite. Anthracite cathode blocks are no longer used in aluminum smelters due to their high electrical resistance and higher energy consumption. The modeled thermal-mechanical stress due to the expansion at the top of the cathode panel while the bottom of cathode blocks is held stationary by steel collector bars after 20 hours of cooling is > 11 MPa, which is sufficiently high to cause cracks along the length of cathode blocks.

Thus, aluminum cells are not damaged due to cooling only 300 degrees, (e.g., from 960 to 660 °C) when power is interrupted up to 8 hours and the cell continue to operate after the potlines is reenergized because:

- The thermal-mechanical stress, (less than 3 MPa) due to thermal gradients in cathode blocks is insufficient to cause fracture of cathode blocks,
- The thermal shrinkage of the length of the cathode panel, (less than 1 cm) is insufficient to cause fracture of cathode blocks,
- The thermal-mechanical stress due to the expansion at the top of the cathode panel while the bottom of cathode blocks is held stationary by steel collector bars, (less than 3 MPa) is insufficient to cause fracture of cathode blocks

The 3D thermal modeling results in this investigation verify that the stress generated in 8 hours, or less, due to cooling as a result of power interruptions is insufficient to cause stress > 8 MPa necessary to cause fractures and cracks in the cathode panel of industrial aluminum cells. Thus, there is no evidence that cathodes are damaged in industrial aluminum electrolysis cells after up to 8 hours of cooling during a power interruption and the cells continued to operate after reenergizing the potline without requiring a shutdown and restart operation.

4. References

1. Xinliang Zhao, Jitai Yan and Bingliang Gao, Restart of 300 kA potline after 5 hours power failure, *Light Metals* 2011, 405-406.
2. Luke Tremblay and Germain Leblanc, Eight-and-half hour power failure and subsequent restart of the 180 kA prebaked aluminum potline in Baie-Comeau, *Production and Electrolysis of Light Metals Proceedings of the Metallurgical Society of Canadian Institute of Mining and Metallurgy*, Halifax, August 20–24, 1989, 29-37.
3. Kayron Lalonde, Wayne Cotton and Richard Beeler, Rate of metal cooling in reduction cell removed from line current, *Light Metals* 2006, 291-295.
4. Ayoola Brimmo, Mohamed Hassan, M.O. Ibrahiem and Youssef Shatillar, Effect of watering and non-watering on the mechanical properties of an aluminium smelter potshell, *Light Metals* 2013, 845-850.
5. Bénédicte Allard, D. Rouby and G. Fantozzi, Fracture behaviour of carbon materials, *Carbon*, 1991, Vol 29, 457-468.
6. Alton Tabereaux, Electrical power interruptions: an escalating challenge for aluminum smelters, *Light Metal Age*, February 2011, 26-32.
7. Bénédicte Allard, Daniel Dumas, Paul Lacroix, Fracture behaviour of carbon materials for aluminum smelters, *Light Metals* 1991, 749-758.

8. Morten Sørli, Harald A. Øye, *Cathodes in aluminium electrolysis*, 3rd Edition, Dusseldorf, Aluminium-Verlag, 2010.
9. Bénédicte Allard, Dreyfus and Michel Lenclud, Evolution of thermal, electrical and mechanical properties of graphitized blocks for aluminum electrolysis cells with temperature, *Light Metals* 2000, 513-521.
10. Bénédicte Allard, Daniel Dumas, F. Durand, G. Fantozzi, D. Rouby, High temperature behaviour of carbon materials used in aluminum smelters, *Light Metals* 1995, 783-790.
11. Donald Picard, Wadii Bouzemmi, Bénédicte Allard, Houshang Alamdari, and Mario Fafard, Thermo-mechanical characterization of graphitic and graphitized carbon cathode material used in aluminium electrolysis cells, *Light Metals* 2010, 832-828.
12. Barry J. Welch, Margert M. Hyland, M. Utley, S.B. Tricklebank and J.B. Metson, Interrelationship of cathode mechanical properties and carbon/electrolyte reactions during start-up, *Light Metals* 1991, 727-733.
13. Jørund Hop, Anee Store, Trygve Foosnaes and Harald Øye, Chemical and physical changes of cathode carbon by aluminium electrolysis, *VII International Conference on Molten Slags Fluxes and Salts*, The South African Institute of Mining and Metallurgy, 2004, 775-781.
14. Marc Dupuis and Alton Tabereaux, Modeling cathode cooling due to power interruption, *Light Metals* 2012, 291-295.
15. Marc Dupuis and Alton Tabereaux, Modeling cathode cooling after power shutdown, *International Aluminium Journal*, 2012, 65-68.